Available online at www.sciencerepository.org

Science Repository

Research Article

α-Mangostin and Doxorubicin Combination Synergistically Inhibited Cell Growth, Induced Cell Apoptosis with Increased Bak Protein and Decreased FLT3-ITD Phosphorylation in AML MOLM-13 Cell Line

Cynthia U. Osemeke, Xuesong Wen, Hemda Garelick and Sandra Appiah*

Department of Natural Science, Faculty of Science and Technology, Middlesex University, The Burroughs, London, UK

ARTICLE INFO

Article history:
Received: 23 July, 2021
Accepted: 11 August, 2021
Published: 30 August, 2021

Keywords:
AML
doxorubicin
α-Mangostin
combination drug
FLT3-ITD
Bak
cdc25

ABSTRACT

Acute myeloid leukemia (AML) is associated with numerous mutations, with the Feline McDonough Sarcoma (FMS) like tyrosine kinase 3 (FLT3) mutation resulting in with poor prognosis and outcome. Therapies have been developed using FLT3 inhibitors, however, drug resistance often leads to disease relapse. In this study, α-Mangostin and doxorubicin (Dox) were evaluated, singly and in combination, for their anti-leukemic effect on MOLM-13, an AML cell line with FLT3-ITD mutation. Cell viability and apoptosis were determined using CyQUANT^{GR} and TUNEL assay, respectively. Cell cycle analysis was conducted on propidium iodide-stained cells using flow cytometry. Cellular proteins were quantified using Western blot technique, with additional study by ELISA for FLT3 kinase activity. The results revealed that cell treatment by the combined drug, Dox (1 μM) and α-Mangostin (20 μM), compared to Dox (1 μM) alone, caused a significant inhibitory effect ($P<0.001$) and indicated synergistic cell growth inhibition. The combined drug also showed increased TUNEL positive apoptotic cells and increased expression of the pro-apoptotic protein Bak compared to Dox alone ($P<0.05$). Dox treated cells, as well as the combined drug induced cell cycle arrest at G_2/M phase compared to untreated cells ($P<0.05$ and $P<0.001$, respectively). There was also statistically significant ($P<0.05$) reduction of cdc25 phosphatases (enzymes which play an important role in G_2/M transition) by the combination drug compared to sole cell treatment by Dox. Furthermore, phosphorylated FLT3 protein expression was reduced when the combined treatment was compared to Dox only after 2 h ($P<0.05$) and after 24 h ($P<0.001$). Thus, Dox and α-Mangostin combined treatment inhibited FLT3 phosphorylation in MOLM-13 cells which could have contributed to G_2M cell arrest and apoptosis via cdc25s and Bak proteins respectively. Further studies are warranted to further evaluate the potential of Dox and α-Mangostin combined drug as inhibitors of FLT3-ITD phosphorylation and its potential clinical relevance in AML treatment.

Introduction

Acute Myeloid Leukemia (AML) is an aggressive blood cancer with fast progression and characterised by poor prognosis with treatment failure due to disease relapse. Although after first line chemotherapy and stem cell transplant, most patients achieve remission, but about 40% develop disease relapse. Following relapse, long term survival is below 20%, median survival is 4-6 months, and this outcome has not improved despite conventional approaches [1]. The success of AML treatment is affected by recurrent genetic and cytogenetic alterations. Among these recurrent alterations, mutations of the Feline McDonough Sarcoma (FMS) such as tyrosine kinase 3 occurs most frequently [2].

FLT3 is a class III receptor tyrosine kinase that plays a crucial role in the proliferation of haematopoietic progenitor cells as well as their differentiation [2]. FLT3 activating mutation may occur either at the juxtamembrane domain (FLT3-ITD) or tyrosine kinase domain (FLT3-

Correspondence to: Dr. Sandra Appiah, Department of Natural Science, Faculty of Science and Technology, Middlesex University, The Burroughs, NW4 4BT, London, UK; Tel: +442084115665; E-mail: S.Appiah@mdx.ac.uk

http://dx.doi.org/10.31487/j.COR.2021.08.12

TKD) [3]. About 30% of newly diagnosed patients with AML carry *FLT3* gene mutation and this mutation is associated with a poor prognosis and a high risk of relapse [2]. Therefore, minimal residual disease (MRD) after chemotherapy is greater in patients with activating FLT3 internal tandem duplication (FLT3-ITD) mutation (23%) while 7% is observed in patients with FLT3-TKD mutation [4]. Although at relapse FLT3-ITD do not always persist, systematic monitoring of patients in first remission for FLT3 ITD mutation remains controversial due to unstable FLT3-ITD positive appearing or disappearing at relapse [4]. The use of FLT3 inhibitors is breakthrough for FLT3 mutation treatment. A multikinase FLT3 inhibitor Midostaurin (Rydapt®) has been approved for newly diagnosed FLT3 patients and gliteritinib, a more specific potent FLT3 inhibitor as monotherapy for relapse/refractory (R/R) AML [3].

However, there is a shorter duration of remission with gliteritinib in R/R FLT3 AML in the absence of allogenic stem cell transplant (ASCT), limited options for refractory patients to gliteritinib therapy and diverse mechanisms of resistance remain ongoing challenges [3]. In addition, pulmonary injury due to treatment with midostaurin [5]. Overall, long term survival with AML remains poor and novel targeted therapies with more effective anti-leukemic activity and reduced toxicity based on new mechanisms of action are needed. There have been reports that continuous phosphorylation by mutant FLT3-ITD affects the activity of cell division cycle 25 (cdc25) phosphatases [6]. Cdc25 phosphatases are cell cycle promoters and are key in regulating mammalian cell cycle; they have also been reported to be involved in the pathogenesis of cancer including myeloid leukemia [6, 7].

Standard therapy for decades in AML treatment have included combination of anthracycline antibiotics such as daunorubicin or doxorubicin (Dox) and cytarabine [8]. The major limitation of Dox or anthracyclines is their dose-related cardiotoxicity and cardiac dysfunction which may be irreversible [9]. α-Mangostin is a major xanthone from the tropical fruit mangosteen, and when studied in leukemic cell lines, it has been reported to have exerted the highest cytotoxicity (compared to other xanthones found in the fruit), reducing cell growth and inducing apoptosis [10]. Chemotherapy drugs often induce cell death via apoptosis, an anti-inflammatory cell death regulated by the tumor suppressor protein p53. Apoptosis is activated either through intrinsic or extrinsic pathways, involving the activation of caspases 3, 8 and/or 9, and apoptotic proteins (including Bax and Bak) and inhibition of anti-apoptotic proteins such as Bcl-2.

An understanding of the role of drug treatments on the effective regulation of the cell cycle and apoptotic proteins is important to help target FLT3-ITD mutation as a potential to prevent relapse or recurrence during treatment of leukemia. In this study, Dox, singly and in combination with α-Mangostin, was evaluated on its cytotoxic effect on MOLM-13 (an AML cell line with FLT3-ITD mutation) and the mechanism of anti-leukemic effect was studied via cellular processes such as apoptosis and cell cycle. Herein, we report a novel finding that the combination of Dox with α-Mangostin caused an inhibition of FLT3 phosphorylation, which in turn resulted in the inhibition of cdc25 phosphatases.

Materials and Methods

I Cell Culture and Reagents

Human AML cell lines MOLM-13 and OCI-AML were obtained from European Collection of Cell Cultures (ECACC) Public Health England. MOLM-13 derived from the peripheral blood of a relapsed acute myeloid leukemic patient with the classification FAB M5 (acute monoblastic leukemia) and the FLT3 mutation, was originally a myelodysplastic syndrome which progressed to AML [11]. OCI-AML2 cell line is established from a 65-year-old man with FAB M4 (acute myelomonocytic leukemia) classification carrying FLT3 wild type and DNMT3A mutation was used as a control for the FLT 3 experiments. Both cell lines were cultured in Roswell Park Memorial Institute (RPMI) 1640 medium (Gibco™ Sigma-Aldrich; Merck, UK), supplemented with 10% fetal bovine serum (FBS, Gibco™ Sigma-Aldrich; Merck, UK), 1% L- glutamine and 1% penicillin/streptomycin antibiotics (Gibco™ Sigma-Aldrich; Merck, UK) at 37°C in a humidified incubator of 5% CO_2, with 2-3 changes of media every week. Viable cells and cell density were determined by staining cells with Trypan blue HyClone® dye (Sigma Aldrich, UK). A 1:1 ratio of cells to dye was counted manually using a haemocytometer under a light microscope. At least 97% of viable cells at logarithmic growth phase were used for assays.

CyQUANT cell assay kit, DeadEnd™ Fluorometric TUNEL system kit was purchased from Promega Corporation (UK), Halt protease inhibitor cocktail, radioimmunoprecipitation assay (RIPA) buffer, Tween-20, phosphate-buffered saline (PBS), dimethyl sulfoxide (DMSO), doxorubicin, α-Mangostin, 0.01% poly-L-lysine, Bradford reagent and FLT3 ligand were purchased from Sigma Aldrich (UK). Phospho-FLT3 Tyr591 was bought from Cell Signaling Technology (UK). VECTASHIELD + DAPI was from Vector Laboratories Inc. (UK). PathScan® Phospho-FLT3 (panTyr) Sandwich ELISA kit #7761C was purchased from Cell Signaling Technology (UK). The primary antibodies for Western Blotting and propidium iodide flow cytometer kit (ab139418) for cell cycle analysis were purchased from Abcam (UK). Secondary anti-rabbit and anti-mouse antibodies, SDS-PAGE gel, nitrocellulose membrane, enhanced chemiluminescent (ECL), horseradish peroxidase (HRP) were from Bio Rad (UK).

II Cytotoxicity Assay: Determination of α-Mangostin and Combination with Doxorubicin (Dox) on Cell Viability Using CyQUANT™ GR

The effect of α-Mangostin, in combination with Dox a chemotherapy drug, was determined on MOLM-13 using CyQUANT™ GR dye. The cells were suspended at a density of 1.5×10^5 cells/ml and plated in 24 well plates, with treatments. After the treatment period (48 or 72 h), the cells were pelleted and frozen at -80°C overnight. The cells were thawed at room temperature, suspended in CyQUANT™ GR buffer and briefly mixed. These suspensions were plated in 96 well plates at (100 µL per well) and allowed to incubate for 2-5 min protected from light and read using microplate reader with fluorescence wavelength of 480 nm excitation and 520 nm emission.

III Apoptosis Assay Using the Fluorescence Microscope

Fragmented DNA of apoptotic cells were measured using fluorometric terminal deoxynucleotidyl transferase dUTP nick end labelling (TUNEL) assay which incorporates fluorescein-12-dUTP at 3'-OH DNA ends using recombinant enzyme terminal deoxynucleotidyl transferase (rTdT) to detect DNA breakage. MOLM-13 cells were seeded at 1.0×10^6 cells/ml in 24 well plate with α-Mangostin (20 µM) singly and in combination with Dox (1 µM) and incubated for 48 h. Slides coated with 0.01% poly-L-lysine and allowed to air dry were used to layer cells collected by centrifugation, for adhesion to the slides. Briefly, cells on the slides were fixed with 4% paraformaldehyde for 25 min and washed twice for 5 min in PBS at room temperature. The slides with cells were then permeabilized with 0.1% Triton X-100 (10 µg/ml) for 5 min then rinsed twice for 5 min in fresh PBS. The slides were incubated with equilibrium buffer (100 µl) for 5-10 min at room temperature, followed by the addition of rTdT incubation buffer (50 µl), and then incubated at 37℃ for 60 min in a humidified chamber. After incubation, the reaction was terminated by immersing the slides in 2X SSC reagent jar for 15 min at room temperature. The slides were washed 2-3 times by immersing in fresh PBS to remove unbound fluorescein-12-dUTP. The labelled end of DNA fragments was stained and mounted in VECTASHIELD + DAPI to stain the nuclei. The slides were then analysed under a fluorescence microscope using fluorescence laser scanning inverted confocal microscope system, Leica TCS Sp5.

IV Cell Cycle Assay

Cell cycle analysis were conducted on MOLM-13 cells seeded at a density of 1×10^6 cells/ml in a 24 well plate treated with α-Mangostin (20 µM) singly and in combination with Dox (1 µM). After 48 h at 37℃, the cells were washed in PBS twice, pelleted and fixed in 70% ethanol for at least 30 min on ice or kept at 4℃. The cells were centrifuged and resuspended with propidium iodide (PI; 400 µl of 50 µg/ml) and RNase A (50 µl of 100 µg/ml) for 30 min in the dark at 37℃. Cell cycle analyses were carried out using flow cytometer [Becton-Dickinson (BD)] fluorescence activated cell sorting (FACS) Calibur flow cytometer) in FL2 channel. The flow cytometer was used to detect the percentage of cells residing in G_0/G_1, S or G_2M phases from DNA content present in the cells.

V Expression of Proteins Using Western Blot Analysis

MOLM-13 cells were treated for 48 h, harvested, washed in cold PBS and kept on ice. The cells were suspended in halt protease inhibitor cocktail (100 µl) and then lysed in RIPA lysis buffer (400 µl) for 20 min on ice, and briefly vortexed every 5 min. The cell lysates were centrifuged at 4℃ and the supernatant collected. The protein concentrations were determined using Bradford assay and 30 µg of proteins were mixed with loading dye, boiled at 95℃ for 7 min, loaded for separation on 12% SDS-PAGE gel and then transferred to a nitrocellulose membrane. The membrane was blocked in 5% BSA 0.1% PBS Tween-20 for 1h and probed with primary antibody at appropriate dilution incubated overnight at 4℃ with gentle shaking. Primary antibodies used included: rabbit monoclonal to active caspase 3 (E83-77), rabbit monoclonal (EPR-362) to p21, rabbit monoclonal to p16 (EPR1473) (all diluted at 1:1000 dilution in 5% BSA in 0.1% PBS-Tween). After incubation the washed membranes were incubated with secondary anti-rabbit antibody1:3000 with 5% BSA in 0.1% PBST for 1 h. Proteins separated on the membranes were visualised using chemiluminescence. The experiments were done in triplicates.

VI Detection of Phosphorylated FLT3 Using Western Blot

FLT3 ligand (FL) was reconstituted in sterile PBS containing 0.1% endotoxin free human serum albumin and used to prepare 100ng/ml working solution. WT-FLT3 cells (OCI-AML) were washed twice in serum free media (RPMI) and incubated in 100ng/mL of FL for 15 min at 37℃. Then cells were washed twice after incubation in cold PBS. Both MOLM-13 and OCI-AML after washing in cold PBS twice were lysed in RIPA buffer for 20 min on ice briefly vortexed every 5 min. Lysates were centrifuged at 14,000rpm for 15 min at 4℃. Protein concentration was determined using Bradford assay and 30 µg of proteins were loaded into the gel, transferred and probed with primary antibody. For FLT3 expression, the membrane was blocked in 5% milk in 0.1% TBS-Tween20 (TBST) and incubated in primary antibody Phospho-FLT3 Tyr591 at 1:1000 in 5% BSA in 0.1% TBST at 4℃ with gentle shaking overnight and secondary antibody 1:3000 with 5% milk in 0.1% TBST. Tyrosine phosphorylation proteins were probed using anti-phosphotyrosine antibody pY20 1:3000 in 5% BSA in 0.1% PBS-Tween20 at 4℃ with gentle shaking overnight. Then secondary antibody1:3000 with 5% BSA in 0.1% PBST for 1 h. Proteins separated on membrane/blot were visualised using chemiluminescence. All experiments were performed in triplicates.

VII Detection of Phosphorylated FLT3 Using Enzyme Linked Immunosorbent Assay (ELISA)

The level of phosphorylated FLT3 was determined using PathScan® Phospho-FLT3 (panTyr) Sandwich ELISA kit #7761C (Tyr589/591). MOLM-13 cell lysates (from 2 and 24 h treated cells) were added into appropriate FLT3 coated antigen micro wells (100 µl/well), sealed and incubated for 2 h at 37℃. The supernatants were then discarded, and the wells were washed four times with 200 µl of 1 X wash buffer. Reconstituted detection antibody (100 µl) was added to each well and the sealed wells were incubated at 37℃ for 1 h. After incubation, the contents of the wells were discarded, and the wells were washed four times with 200 µl of wash buffer. Reconstituted HRP linked secondary antibody was added to each well and the plate with sealed wells were incubated for a further 30 min at 37℃. TMB substrate (100 µl) was added after washing and incubated for 10 min at 37℃. Stop solution (100 µl) was added to each well and the plate was read within 30 min, and the absorbance was read at 450 nm absorbance wavelength.

VIII Statistical Analysis

All data represent mean±SE from at least three experiments. One-way ANOVA with Tukey's post-hoc analysis was used to compare different results obtained and P value < 0.05 was considered statistically significant. Minitab 19 software was used for data analysis. IC_{50} was determined using the GraphPad Prism software. The extent or nature of interaction of two drugs was evaluated using combination index (CI), a universal standard for the analysis of synergism, additive and antagonism. CI was determined using median effect analysis. The

median effect evaluates drug combinations and correlates drug dose and corresponding effect using the equation: CI= d1/D1+ d2/D2 where D1 & D2 are concentration of drug 1 and drug 2 while d1 & d2 is combined concentrations of both drugs [12]. A CompuSyn report was generated that consist of combination index plot with inhibition (Fa) and combination index (CI) values. A CI value of 0.1-0.90 indicates synergism, 0.90-1.10 indicates additive while 1.10-10 indicates antagonistic. The CI value provides a quantitative and mathematical representation of the pharmacological interplay when drugs are combined.

Results

I Cytotoxic and Anti-Apoptotic Effects of α-Mangostin and Doxorubicin, Singly and in Combination on MOLM-13

α-Mangostin (20 µM; IC_{50} value) and therapeutically relevant concentration of Dox (1 µM), singly and combination, were tested to determine their effect on cell viability using CyQUANT^{GR} after 48 h co-incubation with MOLM-13 cells. All the drug treatments significantly ($P<0.05$) inhibited the growth of the AML cells by 50% or less when compared against the vehicle control (DMSO 0.25%) (Figure 1A). More inhibitory effect observed with α-Mangostin and Dox combined drug compared to Dox only ($P<0.001$). CI value of 0.85 was obtained, suggesting possible synergistic effect between α-Mangostin and Dox (Figure 1A).

To determine if cell death was via the induction of apoptosis, the morphological changes in MOLM-13 cells were compared between the vehicle control and drug-treated cells after 48 h treatment. DAPI staining showed cells treated with α-Mangostin to have less apoptotic cells but more of cell fragmentation indicating signs of apoptosis. However, cells in combination treatment showed more apoptotic bodies and less fragmentation (Figure 1B).

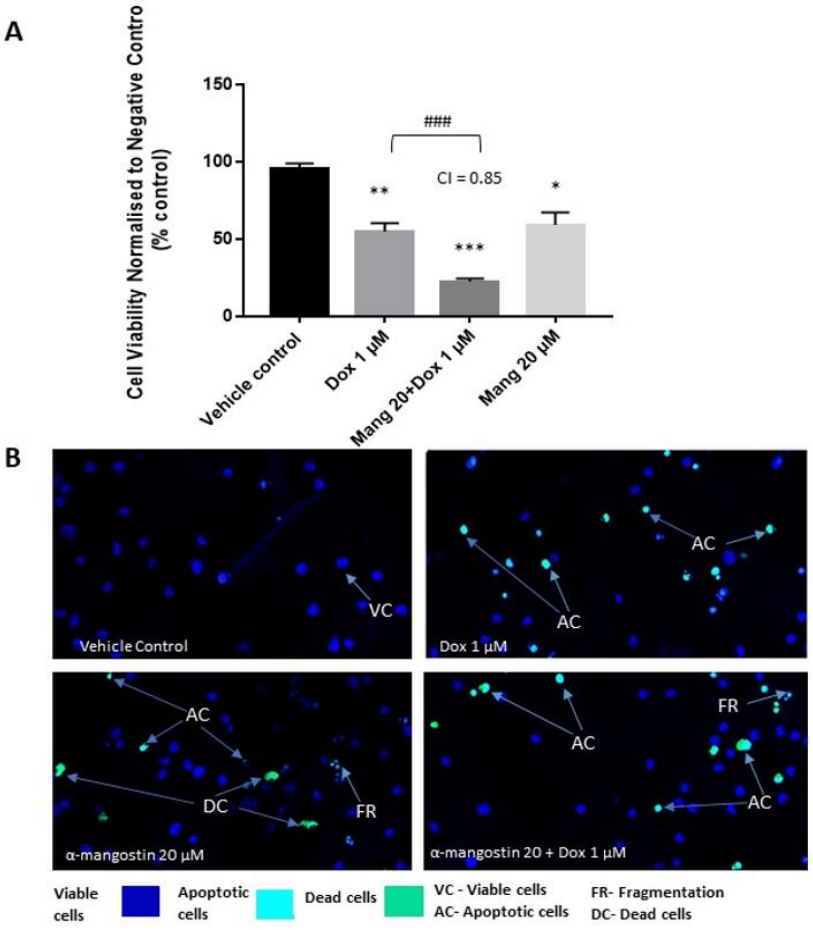

Figure 1: The effect of doxorubicin and α-Mangostin when combined after 48 h treatment in MOLM-13 cell line. **A)** Cell Viability-cells (1.5×10^5 cell/ml) were treated and cell viability was determined using CyQUANT GR. Results were expressed as % control relative to 0.25% DMSO control. Data represent three independent experiments (n=3) with three replicates (n=3 replicates) within an experiment. Statistical analysis was carried out using one-way ANOVA followed by Tukey's post hoc analysis **p<0.01, ***p<0.001 compared to negative control, ## p<0.01 compared to Dox only. IC_{50} of Dox was 1 µM and α-Mang was 20 µM. **B)** The apoptotic effect of doxorubicin and in combination with α-Mangostin in MOLM-13 cells after 48 h using TUNEL assay. Morphology of apoptotic cells was observed. Image is a representative of two independent experiments (n=2) with two replicates within an experiment stained with DAPI and examined with a fluorescence microscope (magnification x200; scale bar 50 µm). Cell reduction and nuclei fragmentation are features of apoptosis.

II Effect of Combination of α-Mangostin and Doxorubicin on Expression of Bcl-2 Family of Proteins and Caspase 3

The expression of pro-apoptotic (Bax, Bak and caspase 3), and anti-apoptotic Bcl-2 proteins were determined using Western blot analysis to elucidate possible mechanisms involved in the cell death observed from α-Mangostin and Dox-treated cells (Figure 2). After 48 h co-incubation of MOLM-13 cells with the combined drug, there was more expression of caspase 3 when compared to single treatments, but this was not statistically significant. However, protein expression of Bak (but not Bax) stimulated by combined α-Mangostin and Dox treatment was statistically significant when compared to Dox only ($P<0.05$).

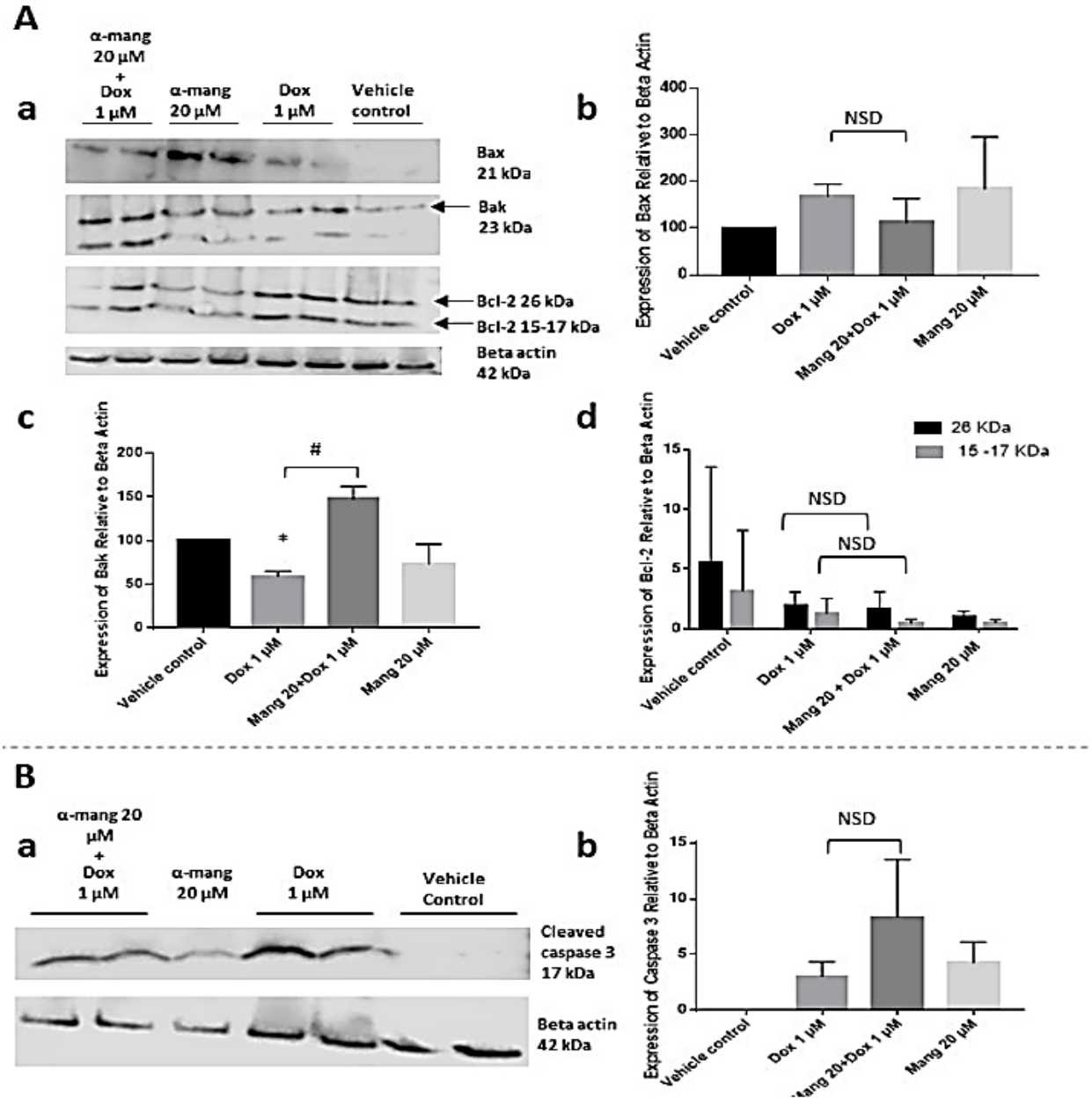

Figure 2: The expression of Bcl-2 family and caspase 3 after 48 h treatment with α-Mangostin singly and in combination with doxorubicin in MOLM-13 cells using Western blotting. **A)** (a) Immunoblotting results of apoptotic proteins (Bax, Bak and Bcl-2) and internal control (housekeeping gene βactin) after treatment with Dox singly and in combination with α-Mangostin in MOLM-13 cells. Cell lysates were subjected to SDS-Page gel for immunoblotting analysis. (b) Graphical presentation of Bax expression. (c) Graphical presentation of Bak expression. (d) Graphical presentation of Bcl-2 expression. **B)** (a) Immunoblotting results of caspase 3. (b) Graphical presentation of caspase 3 expression. Data represent two experiments (n=2) with three replicates (n=3 replicates) (two replicates within an experiment and one replicate from an independent experiment.) for Bax, Bak and Bcl-2. Results were presented as protein expression relative to β-actin ± SD. Statistical analysis was carried out using one-way ANOVA followed by Tukey's post hoc analysis *$p<0.05$ compared to negative control.

NSD: No Significant Difference as indicated.

III Effect of Combination of α-Mangostin and Doxorubicin on the Cell Cycle

The effect of the single and combined drugs on cell cycle was analysed using the Flow cytometer after staining with propidium iodide. α-Mangostin (20 µM) did not show any apparent effect on cell cycle in MOLM-13 cells when compared to vehicle control. Sole treatment of cells by Dox caused accumulation of cells at both the S and G_2/M phases ($P<0.05$; Figure 3). Combination of α-Mangostin and Dox treated cells in G_2/M phase compared to vehicle control showed very strong statistical significance ($P<0.001$; Figure 3). However, G_2M arrest observed with combined α-Mangostin and Dox treatment (31%) was not statistically significant but higher when compared to Dox only treatment (24%) ($P>0.05$; Figure 3).

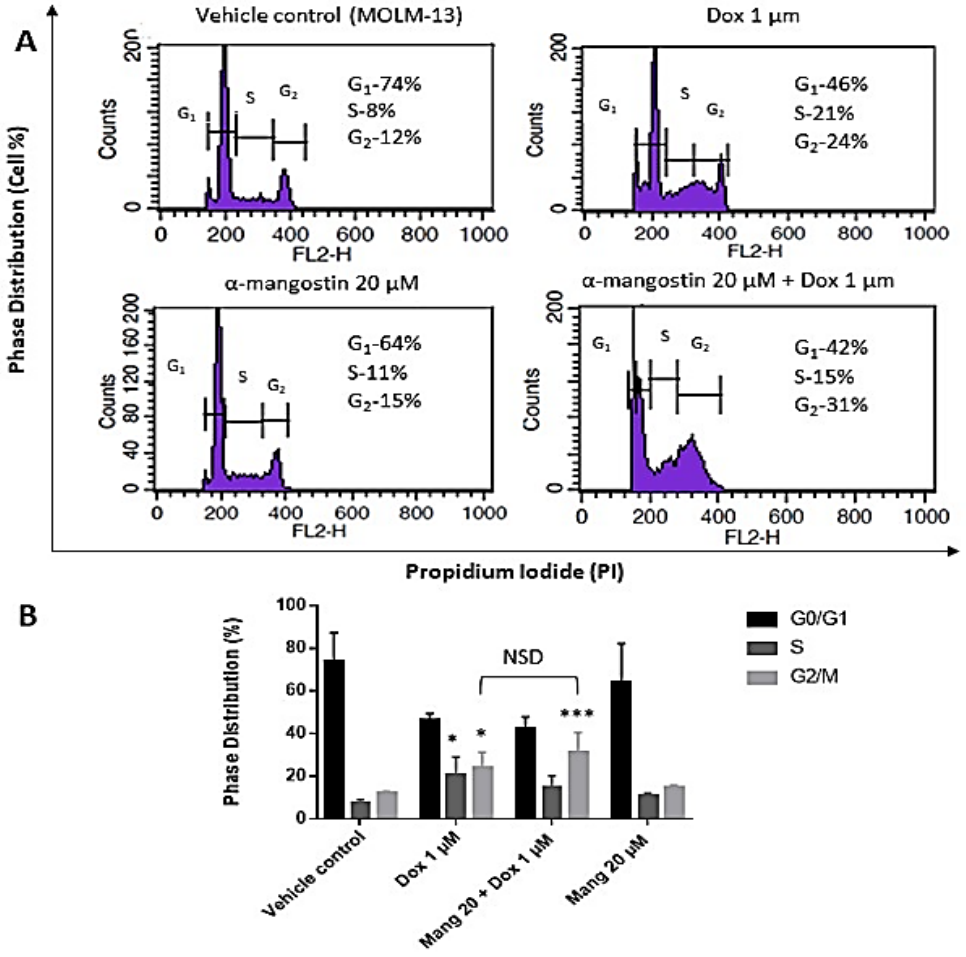

Figure 3: The effect of doxorubicin and α-Mangostin when combined on Cell cycle after 48 h. **A)** DNA histogram showing cell cycle arrest of MOLM-13 cells after treatment with α-Mangostin, and combination of Dox and α-Mangostin for 48 h. The cells were harvested, stained with propidium iodide and analysed using flow cytometer. **B)** Data represent three independent experiments (n=3) with one replicate each (n=3 replicates). Cell cycle distribution was determined as % cell arrest of fluorescence intensity of gated population with linear scaling in G_1, S and G_2/M phase. Statistical analysis was carried out using one-way ANOVA followed by Tukey's post hoc analysis ***$p<0.001$ compared to control.
NSD: No Significant Difference as indicated.

IV Expression of p53, Cell Cycle Arrest Protein p21, cdc25 Phosphatases and Senescence Protein p16 from MOLM-13 Following Combination Treatment of α-Mangostin and Doxorubicin

To determine the mechanism of cell cycle arrest by α-Mangostin and Dox drug combination, p53, p21, and cdc25 phosphatase protein expressions were studied in drug-treated MOLM13-cells after 48 h treatment. The expression of p53 increased two-fold for the combined drug compared to Dox treatment only, but this was not statistically significant (Figure 4). However, strong statistical significance was obtained when the combined drug was compared to the vehicle control ($p<0.01$). When tested on their effect on p21, the combined drug treatment showed non-statistically significant increase of the protein expression by 1.6-fold compared to Dox.

Reduced expression of cdc25 A, B and C after treatment with α-Mangostin and Dox combination was statistically significant when compared to Dox only. Fold-decrease of cdc25 in cells treated with combinational drug treatments were 6.7 for cdc25A ($P<0.05$), 1.7 cdc25B ($P<0.05$), 1.3 cdc25C ($P<0.05$), respectively, when compared to Dox only treated cells.

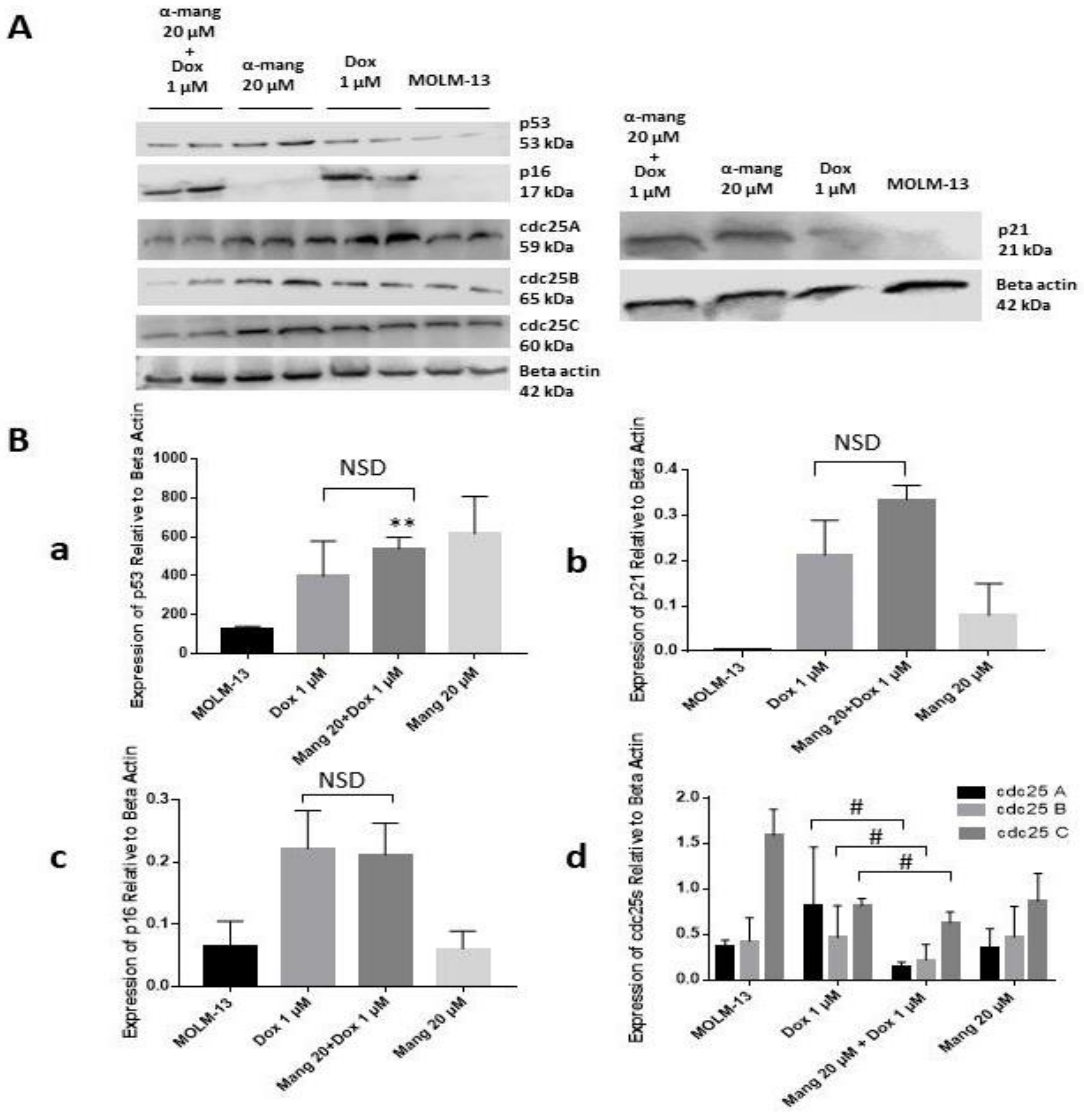

Figure 4: The expression of p53, p21, cdc25s and p16 after 48 h treatment with doxorubicin singly and in combination with α-Mangostin on MOLM 13 cells using Western blotting. **A)** Immunoblotting results of p53, p16, cdc25s and p21 expression after treatment with Dox singly and in combination with α-Mangostin in MOLM-13 cells. Cell lysates were subjected to SDS-Page for immunoblotting analysis. **B)** (a) Graphical presentation of p53 expression. (b) Graphical presentation of p21 expression. (c) Graphical presentation of p16 expression. (d) Graphical presentation of cdc25s expression. Results were presented as % control ± SD of data from two (n=2) experiments with three replicates (n=3) for cdc25A and cdc25B. Two replicates (n=2) within an experiment (n=1) for cdc25C. Three replicates (n=3) for p21 and four replicates (n=4) for p16 expressions relative to β actin due to non-quantifiable protein in control. Statistical analysis was carried out using one-way ANOVA followed by Tukey's post hoc analysis **$p<0.01$ compared to negative control. #$p<0.05$ compared to Dox only.
NSD: No Significant Difference as indicated.

V α-Mangostin and Dox Combination Inhibits Phosphorylation of FLT3-ITD in MOLM-13

To evaluate their effect on FLT3 phosphorylation, 2 and 24 h drug-treated MOLM-13-cells (FLT3-ITD mutant) and OCI-AML2 (wild type FLT3) cell lysates were probed with anti-phosphotyrosine (anti-p-Tyr) and anti- phosphorylated FLT3 (p-FLT3 (Tyr591)) antibodies. Western blot analysis showed that there was reduction of p-FLT3 by α-Mangostin and Dox combination treatment in MOLM-13 cells when compared to either MOLM-13 cells without treatment ($P<0.05$) and Dox only treatment ($P<0.05$) treatment after 2 h (Figure 5A (b)). However, single treatment of either α-Mangostin or Dox alone showed stimulation of p-FLT3 in MOLM-13 but with non-statistical significance. Although co-treatment on MOLM-13 after 2 h showed reduced p-FLT3 when confirmed with ELISA, the reduced p-FLT3 was not significant when compared to vehicle control and Dox only (Figure 5B (a)). However, reduction of p-FLT3 was sustained after 24 h with strong statistical significance obtained when the combined drug was compared to the vehicle control ($P< 0.001$) and Dox only treated cells ($P<0.001$) (Figure 5B (b)).

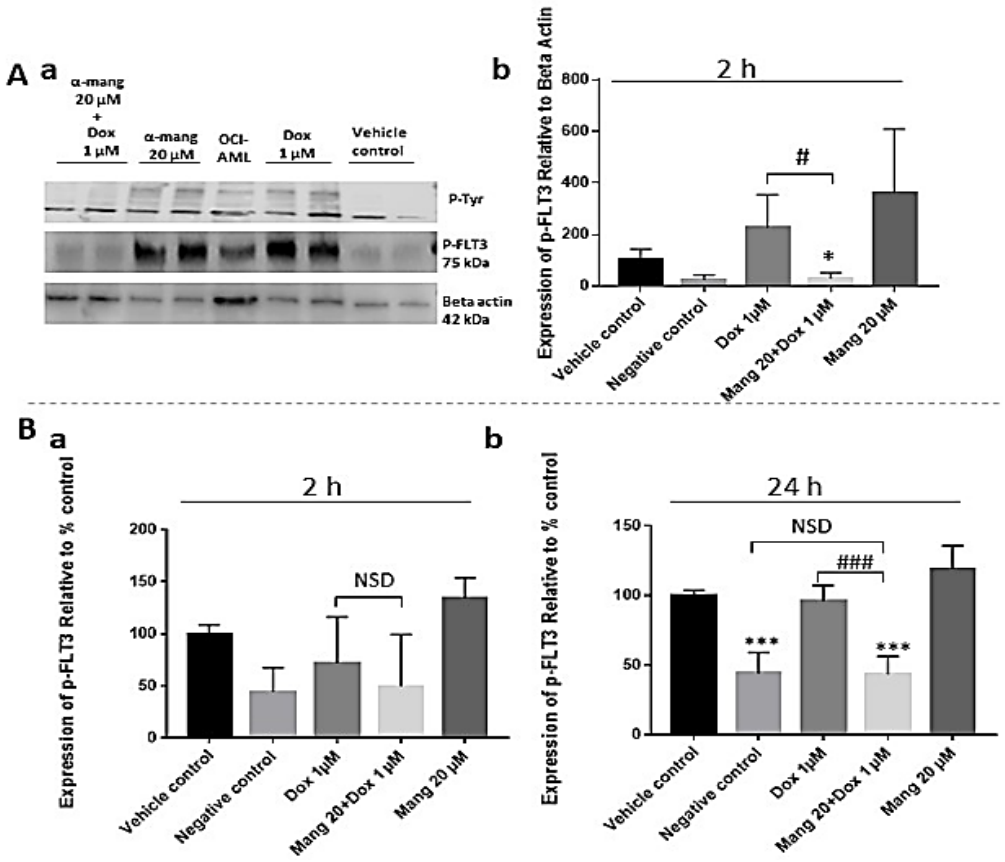

Figure 5: The detection of FLT3-ITD phosphorylation by α-Mangostin and doxorubicin combination after 2 h and 24 h treatment. MOLM-13 cells with FLT3-ITD mutation were treated with α-Mang 20 μM singly and in combination with Dox 1 μM, OCI-AML2 cells were stimulated with FLT3 ligand for 15 min at 37°C. In MOLM-13 cells exogenous ligand was not incubated due to ITD mutation that result in active autophosphorylation of FLT3 with or without ligand binding the FLT3 receptor. Both MOLM-13 and OCI-AML cells were lysed with RPMI and phosphatase inhibitor. **A)** (a) Immunoblot expression of phosphotyrosine (p-Tyr) and phospho-FLT3. (b) Graphical presentation of pFLT3 expression relative to beta actin after 2 hrs using Western blot. **B)** (a) Graphical presentation of phospho FLT3 expression relative to % control after 2 hrs using ELISA, (b) % control phospho FLT3 after 24 h Using ELISA. Data represent two experiments (n=2) with three replicates (n=3 replicates) for Western blot, % control FLT3-ITD ± SD of three replicates (n=3) within two experiments (n=2) for ELISA. Statistical analysis was carried out using one-way ANOVA followed by Tukey's post hoc analysis *$p<0.05$, ***$p<0.001$ compared to MOLM-13 cells, $^{###}p<0.001$ compared to Dox only.
NSD: No Significant Difference as indicated.

Discussion

The genetic heterogeneity of AML accounts for its resistance to therapy. Therefore, targeted therapeutic combinations are strategies necessary for AML treatment. Thirty percent of AML patients harbour FLT3 mutations which are Internal Tandem Duplication (ITD) and Tyrosine Kinase Domain (TKD) occurring in about 23% and 7% of AML patients respectively. A FLT3 mutation can result in full blown leukemia from a state of pre-leukemia [13]. Therefore, FLT3 mutation remains a promising therapeutic target that has gained considerable attention in AML therapy. Currently, newer FLT3 inhibitors such as Gliteritinib are susceptible to resistance which develop due to acquired FLT3 mutation or FLT3 receptor downstream pathways [13].

α-Mangostin is the most abundant compound in the mangosteen fruit was selected due to increasing reports of its anti-cancer effect against cancers including leukemia [14]. In this study, the *in vitro* potential of combined drug; Dox and α-Mangostin on the growth of AML cell line MOLM-13 was compared with the effect of doxorubicin after 48 h exposure. The cytotoxic effect of the drugs was determined and a combination α-Mangostin (20 μM) and Dox (1 μM) and there was an inhibition of cell growth with very strong statistical significance ($p<0.001$) compared to vehicle control and this indicated synergism (combination index = 0.85). Similar synergistic effect was also observed with glioma cells (brain cancer) when nano delivery of α-Mangostin and Dox combination caused an inhibition of tumor growth and prolonged survival time without toxicity [15]. In addition, additive effect but not synergistic effect was observed in multicellular tumor spheroids (MCTSs) from MCF-7 breast cancer cells with the combined drug of α-Mangostin (12 μM) and Dox (12 μM) [16]. Therefore, indicating inhibition of different cancer cells with the combined drug.

There are different possible mechanisms to explain the inhibition of cell viability with Dox and α-Mangostin when combined. The mechanism of

action of Dox includes DNA damage as it intercalates DNA, a topoisomerase II inhibitor, mitochondria targeting and generation of free radicals [17]. α-Mangostin has been reported to diminish topoisomerase I and II to inhibit DNA synthesis and chromosomal segregation proteins [18]. Moreover, it has been reported that Dox supported α-Mangostin by inhibiting PARP1 and PARP2 which are enzymes that protect cells from DNA damage by activating DNA repair process [16]. Therefore, reducing these enzymes could signal for cell damage by α-Mangostin which inhibit topoisomerase II by binding directly and not stabilizing a topoisomerase II- DNA complex [16]. Thus, the suppression of cell growth by the combined drug leading to apoptosis.

A balance between pro-apoptotic proteins (such as Bak, Bax and caspases) and anti-apoptotic proteins (such as Bcl-2) contribute significantly to cell apoptosis or survival. It has been that reported that an upregulation of Bax and downregulation of Bcl-2 in glioma cells treated with Dox and α-Mangostin sole treatment, but not report the effect for the combined drug [15]. Interestingly, in our study, compared to the single drugs, the combined Dox and α-Mangostin showed more Bak protein expression with statistical significance ($P<0.05$), suggesting a contribution of Bak to the enhanced apoptosis induction by the combined drug. Also in our study, reduced Bcl-2 or increased caspase 3 protein expression by all the test drugs were not statistically significant when compared to untreated cells.

In this study, α-Mangostin and Dox combined drug blocked the cell cycle in addition to apoptosis induction, contributing to reduction in cell growth. Cell cycle dysregulation is a hallmark of cancer and the machinery of cell cycle regulation is linked to cellular events such as proliferation, differentiation and apoptosis [19]. There was G_2M phase cell cycle arrest by α-Mangostin and Dox combined drug in this study, with very strong statistical significance when compared to vehicle control ($P<0.001$). Dox is a known DNA damaging agent and, in this study, arrested cells in S and G_2M phase which could contribute to apoptosis induction. Combined α-Mangostin and Dox drug has recently been reported to suppress proliferation of glioma cells with blockage of cell cycle in S phase by expression of p21 and p53 [15]. In the currently reported study, the expression of p53 and p21 was also observed with the combined drug, however, compared to Dox only treatment p53 and p21 were not statistically significant. P53 is a guardian of the genome and modulates cell cycle by targeting p21 a cyclin dependent kinase inhibitor that act on Cdk/cyclin complex to block cells in the cell cycle [20]. Therefore the synergistic effect of α-Mangostin and Dox on MOLM-13 cell cycle arrest at G_2M may suggest a suppression of cyclin dependent kinase (Cdk/cyclin) kinase activity. However, this was not tested in our study. Nevertheless, it is known that when there is cellular Cdk/cyclin complex arrest at G_2M, it is due to DNA damage and the apoptosis pathway is triggered [21, 22].

Cdc25 phosphatases are involved in the dephosphorylation of cyclin dependent kinase (cdk) for the progression of cells in the cell cycle. Cdc25 can be activated by FLT3 to ensure progression of AML cells in the cell cycle. In the current reported study, the combination treatment showed reduced expression of all cdc25s (cdc25A, cdc25C and cdc25C) with statistical significance ($P<0.05$) when compared Dox only. Moreover, compared to Dox only, there was significant reduction of p-FLT3 with the combination treatment after 2 h ($p<0.05$) and very strong inhibition ($P<0.001$) after 24 h. Therefore, suggesting that reduction of p-FLT3 by combination treatment may have resulted in reduced expression of cdc25s in the cell cycle, causing cell arrest at G_2M phase and induction of programmed cell death in MOLM-13. Similar observation has been reported by when combined therapy of Dox and α-Mangostin inhibited growth of glioma cells by promoting apoptosis and blocking cell cycle [15].

α-Mangostin and Dox individual treatment have been reported to inhibit cancer cells and this was observed in this study, and the combination of the drugs enhanced anti-cancer effect. α-Mangostin has been reported to preferentially target cancer cells and not non-cancerous cells thereby suggesting that side effects commonly observed with chemotherapy drugs could be reduced in combination therapy [15, 23]. This requires further investigation to verify. Dox synergistic effect with phytochemicals such as curcumin including α-Mangostin has been reported [15, 24]. Therefore, treatment with two drugs such as Dox and α-Mangostin could enhance efficacy, reduce side effects by lowering the dosage of monotherapy chemotherapy given and further *in vivo* studies are warranted.

In conclusion, this study showed that molecular mechanism of Dox and α-Mangostin combined treatment involves targeting of FLT3 mutation in MOLM-13 which resulted in G_2M phase arrest via inhibition of cdc25 phosphatases (involved in cell cycle) and the induction of apoptosis was via Bak. Further studies are therefore warranted to evaluate the effect of combination drug on signalling pathways (such as STAT5, ERK1/2, P13K/AKT and Ras/MAPK) activated by aberrant signalling of FLT3-ITD receptor. Future work should also endeavour to include known FLT3 inhibitors (for example midostaurin) for comparison study with the combination Dox and α-Mangostin, to investigate as targeted therapy for FLT3-ITD mutation.

Author Contributions

Cynthia Osemeke, Xuesong Wen, Hemda Garelick and Sandra Appiah design, review and finalised the manuscript. Data was collected and analysis was done by Cynthia Osemeke Xuesong Wen and Sandra Appiah.

Acknowledgement

We would like to acknowledge Milan Vu for his support and contributions to the design of the data presentation.

Funding

None.

Availability of Data and Materials

All datasheet used in this study are available when requested for.

Ethics Approval and Consent to Participate

Not applicable.

Consent for Publication

Not applicable.

Competing Interests

None.

REFERENCES

1. Sánchez Corrales YE, Pohle RVC, Castellano S, Giustacchini A (2021) Taming Cell-to-Cell Heterogeneity in Acute Myeloid Leukaemia With Machine Learning. *Front Oncol* 11: 666829. [Crossref]
2. Loschi M, Sammut R, Chiche E, Cluzeau T (2021) FLT3 Tyrosine Kinase Inhibitors for the Treatment of Fit and Unfit Patients with FLT3-Mutated AML: A Systematic Review. *Int J Mol Sci* 22: 5873. [Crossref]
3. Daver N, Venugopal S, Ravandi F (2021) FLT3 mutated acute myeloid leukemia: 2021 treatment algorithm. *Blood Cancer J* 11: 104. [Crossref]
4. Altman JK, Perl AE, Hill JE, Rosales M, Bahceci E et al. (2021) The impact of FLT3 mutation clearance and treatment response after gilteritinib therapy on overall survival in patients with FLT3 mutation-positive relapsed/refractory acute myeloid leukemia. *Cancer Med* 10: 797-805. [Crossref]
5. Paul S, Rausch CR, Jain N, Kadia T, Ravandi F et al. (2021) Treating Leukemia in the Time of COVID-19. *Acta Haematolo* 144: 132-145. [Crossref]
6. Perner F, Schnöder TM, Fischer T, Heidel FH (2016) Kinomics Screening Identifies Aberrant Phosphorylation of CDC25C in FLT3-ITD-positive AML. *Anticancer Res* 36: 6249-6258. [Crossref]
7. Bertoli S, Boutzen H, David L, Larrue C, Vergez F et al. (2015) CDC25A governs proliferation and differentiation of FLT3-ITD acute myeloid leukemia. *Oncotarget* 6: 38061-38078. [Crossref]
8. Dombret H, Gardin C (2016) An update of current treatments for adult acute myeloid leukemia. *Blood* 127: 53-61. [Crossref]
9. Bruynzeel AME, Abou El Hassan MA, Torun E, Bast A, van der Vijgh WJF et al. (2007) Caspase-dependent and -independent suppression of apoptosis by monoHER in Doxorubicin treated cells. *Br J Cancer* 96: 450-456. [Crossref]
10. Matsumoto K, Akao Y, Kobayashi E, Ohguchi K, Ito T et al. (2003) Induction of apoptosis by xanthones from mangosteen in human leukemia cell lines. *J Nat Prod* 66: 1124-1127. [Crossref]
11. Matsuo Y, MacLeod RA, Uphoff CC, Drexler H, Nishizaki C et al. (1997) Two acute monocytic leukemia (AML-M5a) cell lines (MOLM-13 and MOLM-14) with interclonal phenotypic heterogeneity showing MLL-AF9 fusion resulting from an occult chromosome insertion, ins(11;9)(q23;p22p23). *Leukemia* 11: 1469-1477. [Crossref]
12. Chou TC (2018) The combination index (CI < 1) as the definition of synergism and of synergy claims. *Synergy* 7: 49-50.
13. Ambinder AJ, Levis M (2021) Potential targeting of FLT3 acute myeloid leukemia. *Haematologica* 106: 671-681. [Crossref]
14. Ibrahim MY, Hashim NM, Mariod AA, Mohan S, Abdulla MA et al. (2016) α-Mangostin from Garcinia mangostana Linn: An updated review of its pharmacological properties. *Arab J Chem* 9: 317-329.
15. Nie W, Zan X, Yu T, Ran M, Hong Z et al. (2020) Synergetic therapy of glioma mediated by a dual delivery system loading α-mangostin and doxorubicin through cell cycle arrest and apoptotic pathways. *Cell Death Dis* 11: 928. [Crossref]
16. Bissoli I, Muscari C (2020) Doxorubicin and α-Mangostin oppositely affect luminal breast cancer cell stemness evaluated by a new retinaldehyde-dependent ALDH assay in MCF-7 tumor spheroids. *Biomed Pharmacother* 124: 109927. [Crossref]
17. Tacar O, Sriamornsak P, Dass CR (2013) Doxorubicin: an update on anticancer molecular action, toxicity and novel drug delivery systems. *J Pharm Pharmacol* 65: 157-170. [Crossref]
18. Mizushina Y, Kuriyama I, Nakahara T, Kawashima Y, Yoshida H (2013) Inhibitory effects of α-mangostin on mammalian DNA polymerase, topoisomerase, and human cancer cell proliferation. *Food Chem Toxicol* 59: 793-800. [Crossref]
19. Todd R, Hinds PW, Munger K, Rustgi AK, Opitz OG et al. (2002) Cell cycle dysregulation in oral cancer. *Crit Rev Oral Biol Med* 13: 51-61. [Crossref]
20. Feroz W, Sheikh AMA (2020) Exploring the multiple roles of guardian of the genome: P53. *Egypt J Med Hum Genet* 21: 49.
21. Selvarajah J, Elia A, Carroll VA, Moumen A (2015) DNA damage-induced S and G2/M cell cycle arrest requires mTORC2-dependent regulation of Chk1. *Oncotarget* 6: 427-440. [Crossref]
22. De Zio D, Cianfanelli V, Cecconi F (2013) New insights into the link between DNA damage and apoptosis. *Antioxid Redox Signal* 19: 559-571. [Crossref]
23. Johnson JJ, Petiwala SM, Syed DN, Rasmussen, JT, Adhami VM et al. (2012) α-Mangostin, a xanthone from mangosteen fruit, promotes cell cycle arrest in prostate cancer and decreases xenograft tumor growth. *Carcinogenesis* 33: 413-419. [Crossref]
24. Karavasili C, Andreadis DA, Katsamenis OL, Panteris E, Anastasiadou P et al. (2019) Synergistic Antitumor Potency of a Self-Assembling Peptide Hydrogel for the Local Co-delivery of Doxorubicin and Curcumin in the Treatment of Head and Neck Cancer. *Mol Pharm* 16: 2326-2341. [Crossref]